Eur. Phys. J. Special Topics **225**, 147–157 (2016)

DOI: 10.1140/epjst/e2016-02623-x

THE EUROPEAN PHYSICAL JOURNAL SPECIAL TOPICS

Regular Article

Dynamics of ensemble of inhibitory coupled Rulkov maps

T.A. Levanova[1,a], A.O. Kazakov[2], G.V. Osipov[1,3], and J. Kurths[1,3,4]

[1] Lobachevsky State University of Nizhny Novgorod, Nizhny Novgorod 603950, Russia
[2] National Research University Higher School of Economics, Nizhny Novgorod 603155, Russia
[3] Institute of Applied Physics, Russian Academy of Sciences, Nizhny Novgorod 603950, Russia
[4] Potsdam Institute for Climate Impact Research, Potsdam 14473, Germany

Received 24 August 2015 / Received in final form 14 January 2016
Published online 29 February 2016

Abstract. The motif of three inhibitory coupled Rulkov elements is studied. Possible dynamical regimes, including different types of sequential activity, winner-take-all activity and chaotic activity, are in the focus of this paper. In particular, a new transition scenario from sequential activity to winner-take-all activity through chaos is uncovered. This study can be used in high performance computation of large neuron-like ensembles for the modeling of neuron-like activity.

1 Introduction

During the last decade there has become available a huge amount of experimental data that testify hypothesis that sequential switchings of activity governs processes in different neuronal systems such as animal sensory [1] and motor [2,3] systems, or high vocal center [4] in the brain of songbirds. This activity also underlies cognitive processes [5,6], e.g., sequential switchings of bursting activity between groups of neurons in the Nudipleura sensory system control its swimming behavior [7,8]. In order to build a mathematical model that enables us to reproduce such important and prevalent type of activity, one may use a stable limit cycle or a stable heteroclinic contour as mathematical image of sequential activity. The main reason underlying the interest in minimal ensembles is their relation to central pattern generators (CPG) phenomena [9]. CPGs are small ensembles consisting of only few neurons coupled with excitatory or inhibitory couplings. They also can produce sequential switchings of different types of activity without any external stimulus and play a crucial role in the movement and rhythm generation.

Studying of the dynamical regimes and bifurcation analysis in the models which reproduce the described phenomena can be helpful for understanding of principles of functioning and information coding in specified neural ensembles.

Using three coupled Rulkov maps, we construct here a minimal motif of three neurons mutually coupled by inhibitory synapses. The Rulkov discrete neuron model

[a] e-mail: levanova.tatiana@gmail.com

was introduced in [10] and later studied and developed in [11–15]. Our modeling takes into consideration basic principles of chemical coupling: (i) presence and absence of postsynaptic element activity depend on the presynaptic element activity level, and (ii) all interactions between cells are inertial because of chemical processes in neurotransmitters. This model is discrete and, therefore, it is rather easy to numerical analysis.

We study different types of activity that can be generated in this motif by governing coupling parameters. In particular, we focus on a sequential activity regime and bifurcations that lead to its occurrence. Other important regimes existing in the system, in particular winner-take-all regime [16,17] and chaotic regime, are also studied. The analysis was performed using the technique of numerical analysis of charts of largest Lyapunov exponent (LLE) [18].

2 The model

In order to built the described motif we take the neuron-like Rulkov map as an isolated element:

$$\begin{aligned} x_{n+1} &= f(x_n, z_n, y_n) \\ y_{n+1} &= y_n + \mu(-x_n - 1 + \sigma) \\ z_{n+1} &= x_n \end{aligned} \tag{1}$$

where x is a fast variable that qualitatively describes fast ionic currents (Na^+ and K^+) in the cell, and, more generally, corresponds to membrane potential. In the one-dimensional map $x_{n+1} = f(x_n, y_n, z_n)$ f is a discontinuous function

$$f(x,y,z) \;=\; \begin{cases} \alpha/(1-x)+y, & x \le 0, \\ \alpha + y, & 0 < x < \alpha + y \;\; and \;\; z \le 0, \\ -1, & x \ge \alpha + y \;\; or \;\; z > 0. \end{cases} \tag{2}$$

It is constructed in a way to reproduce different regimes of neuron-like activity, such as spiking, bursting and silent regimes.

The variable y corresponds to slow ionic currents such as Ca^{2+}. Its equation sets a nonlinear feedback coupling and makes some nonlinear transient processes possible to be modeled.

The variable z corresponds to the dependency between x_{n+1} and x_{n-1}.

According to the neuron-like dynamics of the map it is possible to construct a low-dimensional model of a neuron that is iterated with a time step congruent to the spike duration. The single element model is able to demonstrate different types of neuron-like activity depending on the parameters α which is a control parameter of the map, and σ which sets the non-perturbed state of the three-dimensional map.

In our modeling we take values of $\alpha = 3.9$ and $\sigma = 1$ from the parameter region so that the element demonstrates a regular tonic spiking regime. $\mu = 0.001$ is a small constant that provides slow changes of the variable y. In the phase space for an individual element there is a periodic point of period 4 for these parameters.

In order to build a plausible model for the inhibitory coupling principle, we use as coupling term an additional term in the right parts of Eq. (1)

$$I_n^{ji} = \gamma_{ji} I_{n-1}^{ji} + g_{ji}(x_{rp} - x_n^i)\xi(x_n^j); \tag{3}$$

multiplied by different constants for x_{n+1} and y_{n+1}. Here j is the presynaptic element, and i is the postsynaptic one. The parameter γ_{ji} is a relaxation time of the synapse, $0 \le \gamma_{ji} \le 1$. It defines the part of synaptic current which preserve as in the next iteration. g_{ji} corresponds to the strength of synaptic coupling and are the governing

parameters of the system, $g_{ji} \geq 0$. x_{rp} is a reversal potential that determines the type of the synapse ($x_{rp} = -1.5$ corresponds to the inhibitory synapse, and $x_{rp} = +1$ – to the excitatory one). $\xi(x)$ is a step function

$$\xi(x) = \begin{cases} 1, & if\ x > x_{th}, \\ 0, & else, \end{cases} \tag{4}$$

with the threshold value x_{th} that implements the principle of inhibitory coupling. If the value of the membrane potential x exceeds the threshold value x_{th}, then the presynaptic elements suppress all activity except subliminal oscillations in the postsynaptic element in case of nonzero coupling.

Finally, the discrete equations that describe a motif consisting of 3 Rulkov elements with synaptic reciprocal couplings are

$$\begin{aligned} x^i_{n+1} &= f(x^i_n, z^i_n, y^i_n + \frac{\beta_{syn}}{2} \sum\nolimits_{j \neq i} (I^{ji}_n)); \\ y^i_{n+1} &= y^i_n + \mu_i(-x^i_n - 1 + \sigma_i \frac{1}{2} \sum\nolimits_{j \neq i} (I^{ji}_n)); \\ z^i_{n+1} &= x^i_n; \\ i &= 1, 2, 3. \end{aligned} \tag{5}$$

In our study we assume that all parameter values for clockwise couplings $g_{12} = g_{23} = g_{31} = g_1$, $\gamma_{12} = \gamma_{23} = \gamma_{31} = \gamma_1$, and for anti-clockwise couplings $g_{21} = g_{32} = g_{13} = g_2$, $\gamma_{21} = \gamma_{32} = \gamma_{13} = \gamma_2$ are equal. Also we assume $x_{rp} = -1.5$, $\beta_{syn} = 0.0001$.

To summarize, we study dynamics of the motif depending only on the strength of synaptic couplings g_i and the relaxation time of the synapse γ_i, $i = 1, 2$ in both cases.

3 The analysis

In order to study and classify the dynamical regimes in the ensemble, we have calculated charts of the largest Lyapunov exponent (LLE) on the parameter plane $P = (g_1, g_2) : g_i \in [0, 10]$, divided into 200×200 nodes. The detailed description of calculating of the LLE charts can be found, e.g. in [18–20].

Let us describe this algorithm in a few words. At each point in P we started a trajectory of the system (5). To accelerate the convergence to the steady-state dynamical regime and due to the multistability of the system in sense of coexisting of several attractors in its phase space for the pair of (g_1, g_2) coupling values, the initial conditions in the internal points of the grid were chosen by using an inheritance scheme which implies that the state obtained by applying the algorithm in the previous point was used as the initial point in each subsequent point of the grid. Note that in all experiments we use the inheritance scheme from the right boundary of the grid to the left. To preclude a transient process we performed 10^5 preliminary iterates of the system (5) and then the largest Lyapunov exponent was estimated on the 10^6 interval by the Benettin method [21]. As a result of the calculations, the pixels on the charts have the following colors: if the LLE < 0 (a limit regime corresponds to the cycle of some period) a color tone is blue and if LLE > 0 (a limit regime corresponds to chaotic attractor) a color tone is yellow.

Figure 1 shows charts of LLE for different values of parameter $\gamma_1 = \gamma_2$ that corresponds to the synapse relaxation time. The charts are symmetrical regarding the line $g_1 = g_2$ as a result of the invariance of the system with regard to substitution of the coupling values g_1 and g_2.

Note that on the constructed LLE charts we mark different regimes (depending on the LLE, level of activity of each element, interspike intervals and presence of burst)

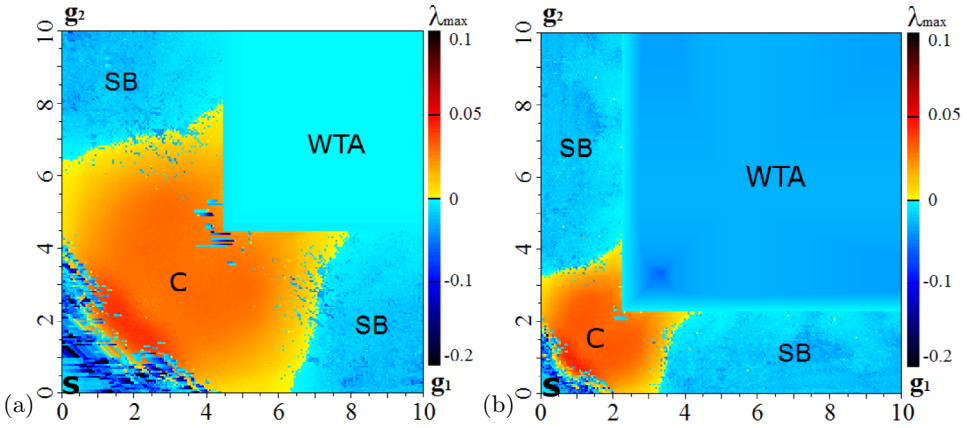

Fig. 1. LLE charts of the system (5). Different regimes of neuron-like activity are marked by the following abbreviations: SB – the region of sequential bursting dynamics, S – the region of spiking activity, WTA – the region of winner-takes-all regimes, C – chaotic region. (a) $\gamma_1 = \gamma_2 = 0$ (b) $\gamma_1 = \gamma_2 = 0.5$.

using the following abbreviations:

(i) SB – sequential bursting activity;
(ii) S – regular spiking activity;
(iii) C – chaotic spiking activity;
(iv) WTA – winner-take-all activity.

As one can see from Fig. 1, the SB regime is observed in the case of strong asymmetry of couplings, the WTA regime – in the case of exceeding of some threshold by values of both couplings. These results well agree with previous investigations of motifs consisting of inhibitory coupled elements, see [22–25] and references therein. The S regime is observed for quite small values of both couplings. It was observed in numerical experiments that all of these regimes are multistable, i.e. several stable periodic points of different periods coexist in the phase space of the system, and depending on the initial conditions the phase point is attracted to one of them. There is also a wide region of chaotic activity (C regime) with regular domains inside it.

It was shown, that increasing of the parameter γ_1 (or γ_2) leads to a shift of the borderlines, which divide the region of different regimes, in the direction that corresponds to the zero value of the coupling g_1 (g_2). It was demonstrated that increasing of the relaxation time almost does not change the types of activity by itself. It only decreases the level of subliminal activity in the suppressed elements in the case of the WTA regime.

The evolution of LLE along the lines $g_2 = 1$ and $g_1 = g_2$ is shown in Fig. 2. Both pictures were obtained using the previously described inheritance scheme. These diagrams show the dependency between LLE and the coupling parameters g_1 and g_2 and provide more information about attracting sets in the phase space of the system (5) as well. Continuous changes of LLE mean that the phase point goes to the same attracting set during the changing of a coupling parameter, and gaps between LLE values for neighboring values of a coupling parameter means that the phase point was attracted to different attracting sets because of the destruction of the previous attracting set or an extremely shrinking of its attraction basin. In the Fig. 2a one can see two regions of with regular attractors (periodic points of different period), which appears and destroys with varying of the coupling parameter g_1: the first region is $0 < g_1 < 1.87$ and the second region is $g_1 > 7$. In Fig. 2a there are also two regularity

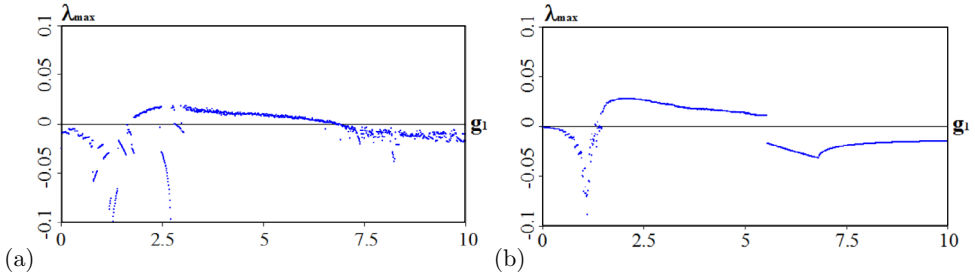

Fig. 2. LLE for the chart from Fig. 1a depending on the coupling values g_1 and g_2: (a) g_1, $g_2 = 1$ (b) $g_1 = g_2$ of the system (5).

windows including periodic points of different periods near the value $g_1 = 2.5$ inside the chaotic dynamics region that correspond to the segment of positive LLE. As one can see, the transition from chaos to regular regimes in this case is quite smooth. In Fig. 2b one can see the evolution of the LLE along the line $g_1 = g_2$ in the map of LLEs (Fig. 1a). It is quite similar to Fig. 2a, except of a hard transition from chaos to multistable WTA regimes near $g_1 = 5.45$. After this transition we observe two regions of smooth changing of LLE divided by a non-smooth transition at $g_1 = g_2 = 7$. Jumping to another periodic point occurs due to shrinking of the attraction basin of the current periodic point.

The next subsections present a more detailed study of the specified dynamical regimes. In the following study we take $\gamma_1 = \gamma_2 = 0$.

3.1 Sequential bursting activity (*SB* regime)

In this study we are most interested in the SB regime that is observed in the system for a strong asymmetry of couplings. Then one of the governing couplings value, e.g., g_1, is sufficiently large, but the others, e.g., g_2, is extremely small or equal to zero. This condition provides a reproduction of the SB regime that is characterized by the following features: (i) all elements in the ensemble are sequentially activated, (ii) an element generates tonic spikes when it is active, and (iii) periods of activity have the same length for all 3 elements.

We find that depending on the period of the stable periodic point main features of the sequential activity regimes differ in the following way:

- Sequential activity with equal interspike intervals inside bursts are associated with stable periodic points of periods about 50–150 (Fig. 3(a)). It can be observed mostly in case of proximity to zero of one of the couplings‘ values.
- Sequential activity with unequal interspike intervals inside bursts are associated with stable periodic points of very high periods (Fig. 3(b)). Also periods of activity of adjacent elements have intersections. This fact can be attributed to the following: in the projection of the 9-dimensional phase space to the 3-dimensional subspace (x_1, x_2, x_3) for high periodic points of period k there exist some $k_1 < k$, such that the k_1-th image of the point is closer to the x_{i+1} axes, while most previous images of the point lie near the x_i axes that corresponds to the x_i activation. As the period of the periodic point sufficiently increases, the LLE in this case becomes close to zero but still remains negative (the largest Lyapunov exponent $\lambda_{max} \approx -0.004$).

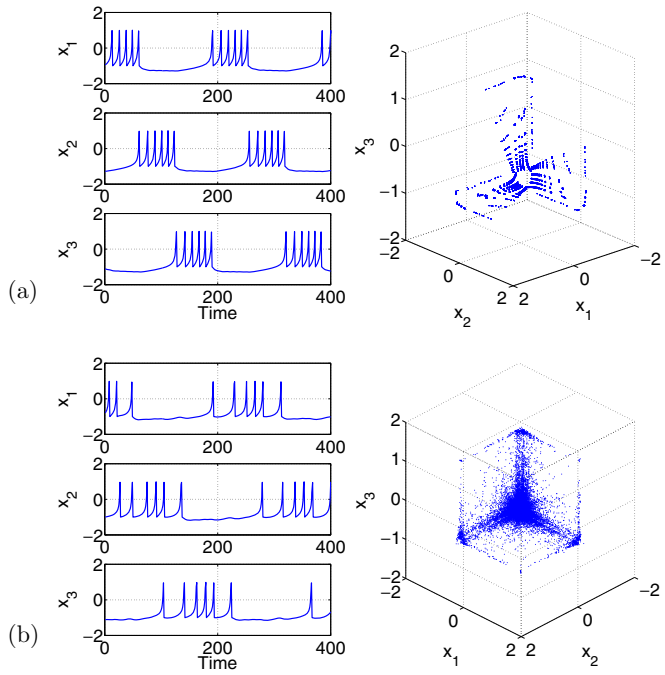

Fig. 3. (a) Time series of x_1, x_2, x_3 and he projection of phase space of system (5) to the 3-dimensional subspace (x_1, x_2, x_3) in the case of sequential activity with equal interspike intervals, $g_1 = 0$, $g_2 = 7$; (b) Same as in (a) but for $g_1 = 1$ and with unequal interspike intervals.

3.2 Spiking activity (*S* and *C* regimes)

Figure 1 shows that there exists a region of spiking activity of different type, including spiking activity with constant intervals between spikes of different elements (see Fig. 4(a)) and spiking activity with different intervals between spikes of different elements (see Fig. 4(b)).

As in the case of SB regime, the corresponding value of the period of the stable periodic point defines the type of the spiking regime. If the period is quite small, the spiking process looks like a sequential activation of elements with constant intervals between spikes that depends on initial conditions. With increasing of the period of the stable periodic point the time between spikes in each element becomes slightly different and the time series look as for non-regular case despite the fact that analysis shows a regular nature of this regime.

In the case of small couplings the regime may look similar to the regime in the case of uncoupled oscillators, so let us briefly describe the main features of the influence of small coupling on the dynamics of the system (5). Even for small values of parameters g_1 and g_2 (for example $g_1 = 0.05$, $g_2 = 0$) the phase space of the system changes: instead of a periodic point of period of 4 (as it was found in [10]), which corresponds to the case of tonic spiking in uncoupled oscillators, a periodic point of higher period appears. Therefore the amplitude of spiking becomes smaller (upper bound of the value of membrane potential takes the value of 1 instead of 1.5 as in case of uncoupled elements), and the spiking frequency also becomes lower.

In a wide region of coupling parameter values chaotic spiking activity is observed (see Fig. 5). In contrast to the previous case of spiking activity that only looks like

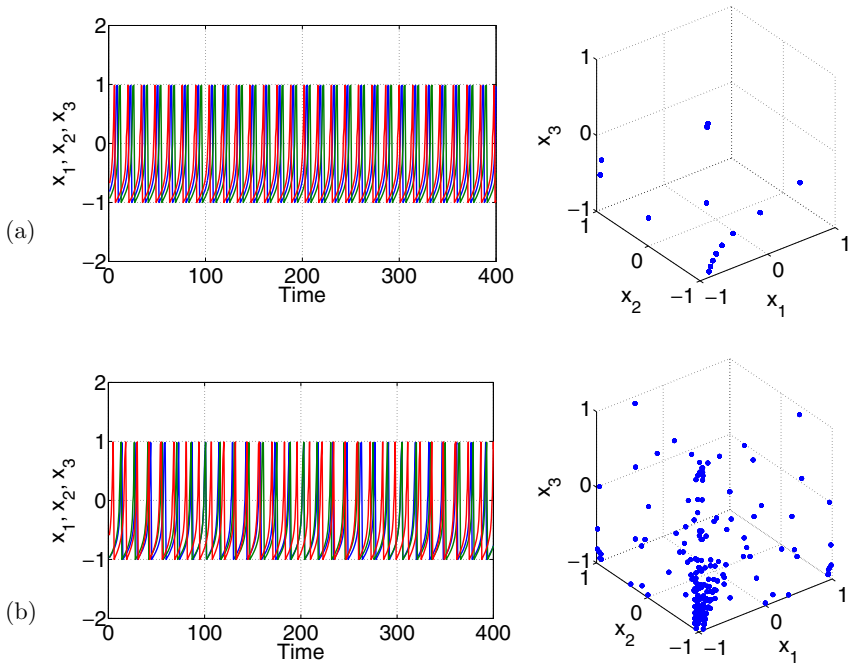

Fig. 4. Time series of x_1, x_2, x_3 and the projection of phase space of system (5) to the 3-dimensional subspace (x_1, x_2, x_3) in case of spiking activity (a) $g_1 = 1$, $g_2 = 0$ (b) $g_1 = 1$, $g_2 = 1$. LLE is negative in both cases: (a) $\lambda_{max} \approx -0.0509$ (b) $\lambda_{max} \approx -0.1086$.

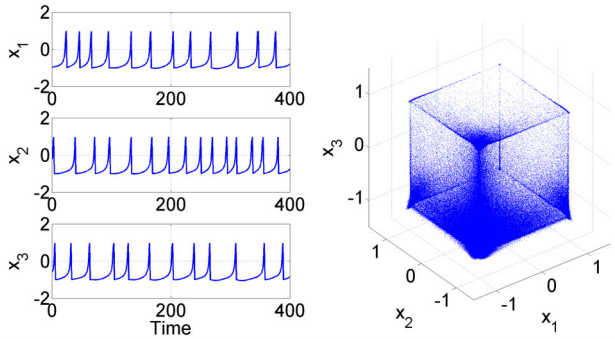

Fig. 5. Time series of x_1, x_2, x_3 and the projection of phase space of system (5) to the 3-dimensional subspace (x_1, x_2, x_3) in case of chaotic spiking activity for coupling values $g_1 = 3.1$, $g_2 = 3$, the largest Lyapunov exponent $\lambda_{max} \approx +0.05$.

non-regular (interspike intervals are non-equal, LLE is close to zero but remains negative), in this case the LLE is positive.

As it can be seen from Fig. 1, in the regions of chaotic regimes there are some domains of regularity, which, generally speaking, are typical for nonhyperbolic chaos [26].

3.3 Winner-take-all activity (*WTA* regime)

In a wide region of coupling parameters g_1 and g_2 different WTA regimes coexist. Depending on the initial conditions one of the elements in the motif demonstrates

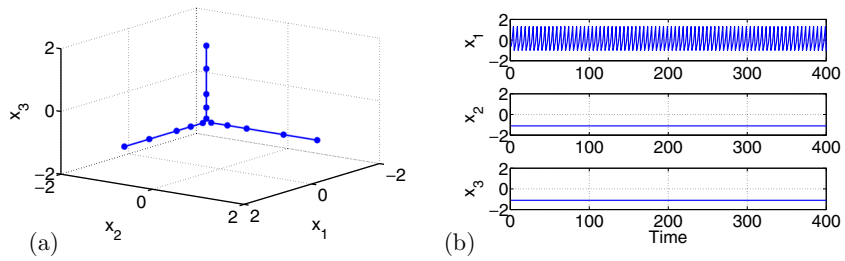

Fig. 6. (a) Coexistence of three periodic points of the period of 5 in the projection of the 9-dimensional phase space of system (5) in the 3-dimensional subspace (x_1, x_2, x_3) in case of multistable WTA regimes. Each periodic point corresponds to the WTA regime when the corresponding element demonstrates tonic spiking activity and others are suppressed; (b) Time series of x_1, x_2, x_3 in the case when the phase point was attracted to the one of the periodic points of period 5.

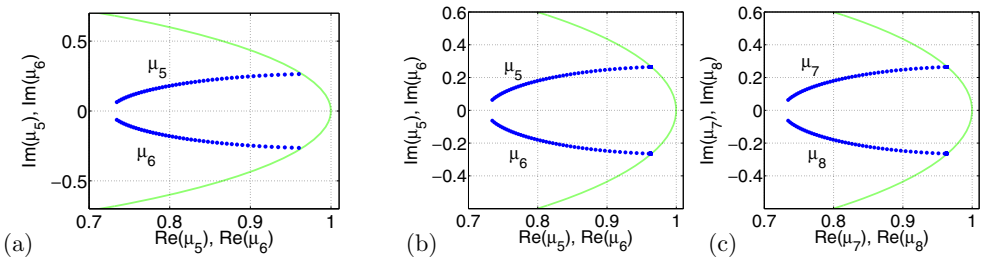

Fig. 7. (a) Subcritical Neimark-Sacker bifurcation of a triplet of periodic points: two complex-conjugated multipliers μ_5 and μ_6 (blue dots) of the periodic point of period 4 cross the unit circle (green curve), $g_2 = 7$, g_1 variates from $g_1 = 7$ to $g_1 = 4.99$ (b) Double subcritical Neimark-Sacker bifurcation of the triplet of periodic points of period 4: two pairs of complex conjugated multipliers (μ_5, μ_6) and (μ_7, μ_8) (blue dots) of the corresponding periodic point cross the unit circle (green curve), the coupling values variate from $g_1 = g_2 = 7$ to $g_1 = g_2 = 4.99$. In both cases other multipliers remain inside unit circle.

tonic spiking while others are suppressed to the level of subliminal activity. In the phase space of the system (5) three triplets of periodic points of periods 4, 5 and 6 coexist (see Fig. 6 for the triplet of periodic points of period 5). A larger period of the periodic point corresponds to lower spiking.

3.4 Bifurcation analysis

In this section we study bifurcations which lead to the transition from multistable regimes of winner-take-all activity to chaotic activity and sequential switching activity. To perform bifurcation analysis we calculate multipliers of periodic points (see Fig. 7). We perform the following experiment: fix the coupling value $g_2 = 7$, and start to decrease g_1 from the initial value $g_1 = 7$. We find that in this case triplets of periodic points of periods 4, 5 and 6 sequentially bifurcates via a subcritical Neimark-Sacker bifurcation, when the coupling parameter reaches the threshold values for each triplet of periodic points.

The triplet of periodic points of period 4 collapses first when g_1 reaches the threshold value $g_1 = 4.99$ (see Fig. 7(a)), and the triplet of unstable cycles, which can not be observed in numerical experiments because of the non-reversibility of the dynamical

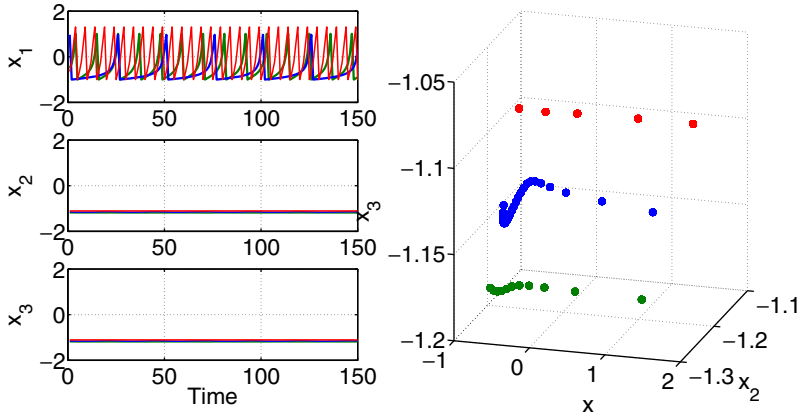

Fig. 8. Time series for the variables x_1, x_2, x_3 and the projection of the 9-dimensional phase space of system (5) to the 3-dimensional subspace (x_1, x_2, x_3) in case of WTA dynamics for different values of σ_i, $i = 1, 2, 3$, coupling values were taken equal to $g_1 = g_2 = 7$: red color corresponds to $\sigma_1 = \sigma_2 = \sigma_3 = 1$, green color to $\sigma_1 = \sigma_2 = \sigma_3 = 0.5$, and blue color to $\sigma_1 = \sigma_2 = \sigma_3 = 0.3$. Decreasing of σ_i leads to a slowing down of the spiking process and increasing of the period of the correspondent periodic point in the phase space. Further decreasing of σ_i, $i = 1, 2, 3$ leads to the appearance of chaos in all individual elements of the system (5).

system, appears. Further near $g_1 = 4.85$ on the same scenario triplet of stable periodic points of period 5 collapses. When g_1 reaches the third threshold value $g_1 = 4.49$, the last triplet of periodic points of period of 6 collapses via a subcritical Neimark-Sacker bifurcation. After this last bifurcation one does not observe the winner-takes-all regimes in the system but only finds chaotic dynamics.

This result is symmetrical with regard to the substitution $(g_1 \to g_2)$ and $(g_2 \to g_1)$ owing to the symmetry of the system with regard to specified substitution (one can graphically see this fact on the map of the dynamical regimes that is symmetrical with regard to the line $g_1 = g_2$).

A double subcritical Neimark-Sacker bifurcation occurs (Fig. 7(b)) in the case of a similar transition from the region of regimes of winner-takes-all type into the region of chaos along the line $g_1 = g_2$ for the same threshold values and the same sequence of triplets of periodic points of periods 4, 5, 6.

We are interested in transitions near borderlines of regularity domains inside the chaotic region. In this case the attracting basins of stable periodic points near threshold values of its birth and death are very small, and this fact makes numerical studies difficult. It was shown that 2 complex conjugated multipliers of a periodic point near the threshold values on the left border have a tendency to go to the unit circle.

4 One more realistic modeling: Slowing down of spiking in the winner-takes-all regime

As it was shown in [10], decreasing of the parameter σ leads to decreasing of the spiking frequency setting of chaotic dynamics in the individual element. To obtain a more realistic spiking process, especially in the case of WTA dynamics (see Fig. 8), we will study the dependence of the system's dynamics on the parameter σ.

Figure 9 shows that decreasing of parameters σ_i, $i = 1, 2, 3$ for each element in the motif leads to an appearing of the chaotic behavior in the SB region. The region

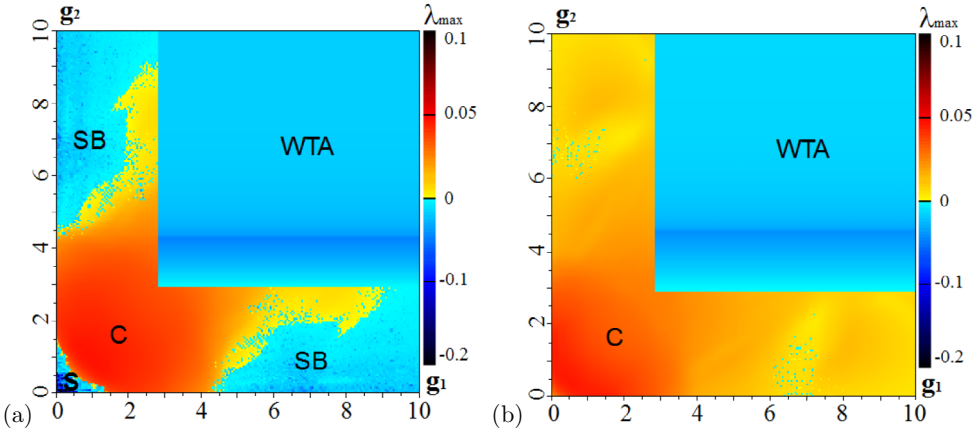

Fig. 9. LLE charts of the system (5). Different regimes of neuron-like activity are marked by the following abbreviations: SB – the region of sequential bursting dynamics, S – the region of spiking activity, WTA – the region of winner-takes-all regimes, C – chaotic region. $\gamma_1 = \gamma_2 = 0$. (a) $\sigma_1 = \sigma_2 = \sigma_3 = 0.5$ (b) $\sigma_1 = \sigma_2 = \sigma_3 = 0.3$.

of SB becomes a region of chaotic activity already in the case of $\sigma_i = 0.4$, i.e. much earlier than the appearing of chaos in the individual element. Also the region of WTA dynamics becomes wider with decreasing of σ_i. This finding leads us to some consensus between decreasing spiking frequency and preserving all types of activity in the ensemble that was described earlier.

5 Conclusion

These investigations continue the study of the impact of inhibitory couplings on dynamics of motifs of neuron-like elements and different transitions from sequential activity to winner-takes-all regimes described in [23–25]. In this paper we study dynamical regimes which may be observed in an ensemble of inhibitory coupled Rulkov elements depending on coupling values. This way, we uncover the new transition scenario from sequential activity to winner-takes-all regimes through chaos. The obtained results give us a possibility to study numerically effects of inhibitory coupled neurons in large ensembles in cases when it is necessary to reproduce phenomena and main features of certain type of activity such as interburst and interspike intervals, regularity of the process etc. Our theoretical findings can be proved by experimental studies, where all specified types of neural activity [27–30] and effects of inhibitory network related to these regimes (see the review [31] and references therein) were observed in experiments. All these cases let us state that using this numerical analysis, we can predict main neural phenomena in ensembles of inhibitory coupled neurons.

Authors acknowledge N.F. Rulkov and S.V. Gonchenko for useful notes and fruitful discussion.

The work was supported by the following grants: results from Sects. 3.1–3.2 were supported by Russian Science Foundation (Contract No. 14 12 00811), results from Sect. 3.3 were supported by the Federal Target Program Research and Development in Priority Areas of the Development of the Scientific and Technological Complex of Russia for 2014–2020 of the Ministry of Education and Science of Russia (Project ID RFMEFI57514X0031 Contract No. 14.575.21.0031), results from Sect. 3.4 were supported by the Government of

the Russian Federation (Agreement No. 14.Z50.31.0033), results from Sect. 4 were supported by the Basic Research Program at the National Research University Higher School of Economics (project 98) in 2016 and by Laboratory of Algorithms and Technologies for Network Analysis, NRU HSE. Numerical experiments were conducted on the computational cluster of the laboratory LATNA of National Research University Higher School of Economics using programmed complex Computer Dynamics: Chaos.

References

1. V.S. Afraimovich, M.I. Rabinovich, P. Varona, Int. J. Bif. Chaos **14**(4), 1195 (2004)
2. M.I. Rabinovich, et al., Biol. Cybern. **95**(6), 519 (2006)
3. P. Varona, et al., Chaos **12**(3), 672 (2002)
4. M.S. Fee, A.A. Kozhevnokov, R.H.R. Hahnloser, Annals NY Acad. Sci. **1016**, 153 (2004)
5. M.A. Komarov, et al., Chaos **19**(1), 015197 (2009)
6. M.I. Rabinovich, et al., PLoS Comput. Biol. **4**(5), e100072 (2008)
7. A. Sakurai, et al., Current Biology **21**, 1036 (2011)
8. J. Newcomb, et al., Proc. Natl. Acad. Sci. **109**, 10669 (2012)
9. E. Marder, R.L. Calabrese, Physiol. Rev. **76**(3), 687 (1996)
10. N.F. Rulkov, Phys. Rev. E **65**, 041922 (2002)
11. A.L. Shilnikov, N.F. Rulkov, Int. J. Bif. Chaos **13**(11), 3325 (2003)
12. A.L. Shilnikov, N.F. Rulkov, Phys. Lett. A **328**, 177 (2004)
13. N.F. Rulkov, I. Timofeev, M. Bazhenov, J. Comput. Neurosci. **17**, 203 (2004)
14. M. Bazhenov, et al., Phys. Rev. E **72**, 041903 (2005)
15. I. Tristan, et al., Chaos **24**, 013124 (2014)
16. C. Blakemore, R.H. Carpenter, M.A. Georgeson, Nature **228**(5266), 37 (1970)
17. G.K. Wu, et al., Neuron **58**(1), 132 (2008)
18. S.P. Kuznetsov, *Dynamical chaos* (Fizmatlit, Moscow, 2001) (in Russian)
19. A.V. Borisov, et al., Regular & Chaotic Dyn. **17**(6), 512 (2012)
20. A.V. Borisov, A.O. Kazakov, I.R. Sataev, Regular Chaotic Dyn. **19**(6), 718 (2014)
21. G. Benettin, et al., Meccanica **15**, 9 (1980)
22. M.V. Ivanchenko, et al., J. Theor. Biol. **253**, 452 (2008)
23. M.A. Komarov, G.V. Osipov, S. Zhou, Phys. Rev. E **87**, 022909 (2013)
24. A.O. Mikhaylov, et al., Europhys. Lett. **101**(2), 20009 (2013)
25. T.A. Levanova, M.A. Komarov, G.V. Osipov, Eur. Phys. J. Special Topics **222**(10), 2417 (2013)
26. V.S. Aframovich, L.P. Shilnikov, *Strange attractors and quasiattractors*, in Nonlinear Dynamics and Turbulence, edited by G.I. Barenblatt, G. Iooss, D.D. Joseph (Pitmen, Boston, 1983)
27. M. Wehr, G. Laurent, Nature **384** (1996)
28. A. Luczak, et al., Proc. Natl. Acad. Sci. USA **104**(1), 347 (2007)
29. J.G. Nicholls, et al., *Neuron to Brain*, 4th ed. (Sinauer Associates, Sunderland, 2001)
30. H. Korn, P. Faure, C.R. Biologies **326**, 787 (2003)
31. C. Assisi, M. Stopfer, M. Bazhenov, Neuron. **69**, 373 (2011)